1

***Abstract*—Radar sensing can be integrated with communication in what-we-call future perceptive mobile networks. Due to complicated signal structure, it is challenging to estimate sensing parameters such as delay, angle of arrival and Doppler when joint communication and radar sensing (JCAS) is applied in perceptive mobile networks. This paper studies radar sensing with signals compatible with fifth generation (5G) new radio (NR) standard using one-dimension (1D) to 3D compressive sensing (CS) techniques under 5G channel conditions. Moreover, we propose a two-dimensional cluster Kronecker CS algorithm for significantly improved sensing parameter estimation in JCAS networks via introducing a prior probability distribution to effectively exploit the cluster structure in multipath channels. Simulation results are provided and we focus the respective advantages and disadvantages of these techniques that validate the effectiveness of the proposed algorithms.**

On Joint Communication and Radar Sensing in 5G Mobile Network by Compressive Sensing

Md. Lushanur Rahman[1], J. Andrew Zhang[1], Xiaojing Huang[1], Y. Jay Guo[1], and Zhiping Lu[2]

I. Introduction

The recently proposed *perceptive mobile network* [1], [2], [3], [4], with a conceptual plot provided in Fig. 1, can provide joint communication and radar sensing (JCAS, also known as RadCom) in one system. On a unified sensing platform, information associated with e.g., human behaviour, moving objects and environmental changes can be extracted from communication signals via sensing parameters. The perceptive mobile network is different from the existing JCAS systems and technologies that combine radar and mobile communications. In the perceptive mobile network, no spectrum needs to be separately allocated for communication and sensing, and the spectrum efficiency will be doubled. This is significantly different to existing spectrum sharing concepts [5] such as in cognitive radio, co-existence of wireless communication and radar system where the two systems are physically separated [6], [7], integrated JCAS system using separately transmitted signals [8], [9] and JCAS system where communication is achieved within an original radar system [10], [11]. Perceptive mobile networks belong to the type of JCAS/RadCom system class, where communication is already very well realized and the main challenge is how to achieve radar sensing functionality within the cellular network by its own radio signal without sacrificing the performance of communications.

Estimation of sensing parameters, such as the delay, angle of arrival (AoA), angle of departure (AoD) and Doppler frequency of multipath signals, is a critical task in perceptive mobile networks. Moreover, there is very limited work on JCAS for large-scale cellular networks. The sensing solutions presented here mainly obtained by handling the significant challenges caused in JCAS by highly complicated mobile signals in clustered multipath propagation channels.

The first challenge for sensing parameter extraction in perceptive mobile networks is due to the sophisticated signal structure. Although existing studies demonstrate the feasibility and potential of JCAS, most of them consider general signal formats, such as simple single carrier and multicarrier modulation [12], and is limited to point-to-point links such as millimeter wave radio for vehicular networks [13]. In [14], preliminary work on using orthogonal frequency-division multiplexing (OFDM) signal for sensing was reported. In [15], sparse array optimization was studied for multiple-input multiple-output (MIMO) JCAS systems. In [16], the multiple access performance bound is derived for a multiple antenna JCAS system.

[1] University of Technology Sydney (UTS), Global Big Data Technologies Centre (GBDTC), Australia; [2] China Academy of Telecommunications Technology (CATT), Beijing, China. Corresponding authors: lushanur.rahman@gmail.com; Andrew.Zhang@uts.edu.au.

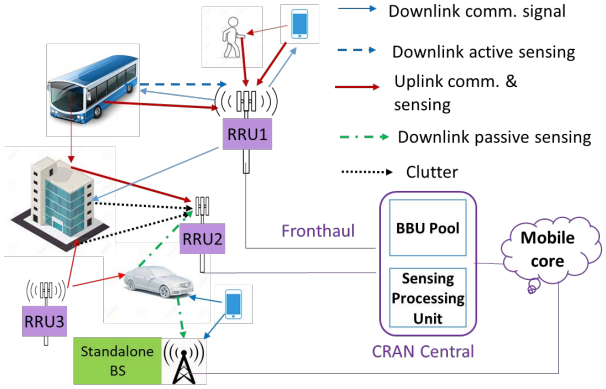

Fig. 1: Proposed perceptive mobile network with 5G CRAN

In [17], mutual information for an OFDM JCAS system is studied, and power allocation for subcarriers is investigated based on maximizing the weighted sum of the mutual information for radar and communications. However, there is only very limited work directly using modern mobile communication signals and networks in JCAS systems, involving orthogonal frequency division multiple access (OFDMA) and multi-user MIMO (aka spatial frequency division multiple access, SDMA). Such signals structure makes most existing sensing parameter estimation techniques not directly applicable. For example, active radar sensing technologies mainly deal with linear FM (LFM) chirp transmitted signals [18]; most passive sensing techniques consider simple single carrier and OFDM signals [19], [20]. In addition, conventional spectrum analysis techniques such as MUSIC [12] and ESPRIT [14] require continuous observations, which are not always available here. In turn, how JCAS can actually be realized at a system level in the mobile network, specifically, how radar sensing can be done based on communication signals using multiuser-MIMO and OFDMA technologies, is a fundamental and challenging problem. In this paper, we deal with compressive sensing (CS) as an excellent candidate technology to solve this problem by developing suitable signal formulation for sensing parameter estimation.

We provide solutions for estimating sensing parameters from 5G NR standard signals in perceptive mobile networks by applying one-dimension (1D) to 3D CS algorithms. These CS algorithms are developed from existing ones to make them capable of estimating all the sensing parameters. We consider both downlink and uplink sensing, to be consistent with downlink and uplink communications. The communication signals used for sensing are the OFDM-type demodulation reference

signals (DMRS) in the 5G specification [21]. We use both 5G-compatible channels recommended by 3GPP and our own generated cluster channel model which has better control for radio propagation for sensing purposes. We compare these CS algorithms, and demonstrate their respective advantages and disadvantages, under various channel conditions and system setup.

The second fact is that practical multipath always arrives in clusters. The multipath signals from one cluster have similar sensing parameters values for delay, AoA and Doppler frequency, and are typically from the same scatter(s). Complexity arises when the clusters originated in a propagation scene may have correlations among other clusters of the same user and across different users due to the same channel condition. Eventually, these create accuracy problems when getting sensing parameters from delay or angle domain without acknowledging channel cluster structure knowledge. Moreover, there are common multipath remains among clusters. There exist research outputs on reconstructing cluster sparse signals in general, for example, through periodic compressive support [22], model based compressive sensing (CS) [23], variational Bayes approach [24], and block Bayesian method [25]. In [26] a millimetre-Wave joint radar and communication system for indoor scenarios is developed, using estimated radar channel coefficients. However, there is only very limited work on how cluster sparsity structure can be exploited in JCAS systems such as perceptive mobile networks that involve OFDMA and multi-user MIMO. Therefore, cluster sparse signal reconstruction for more accurate sensing in perceptive mobile networks, employing OFDMA and multi-user MIMO is our interest.

In this case, we exploit the cluster property in multipath channels through creating a prior probability distribution and propose a novel two-dimensional (2D) CS algorithm for sensing parameter estimation in perceptive mobile networks. In particular, a cluster prior probability density function is introduced in the proposed 2D cluster Kronecker CS algorithm, and shown to efficiently detect the coarse locations of the clusters, leading to more accurate sparse reconstruction performance when Kronecker CS algorithms are applied.

Our major contributions in this paper are as follows:

- We propose an integrated solution built on a unified platform that enables estimating sensing parameters from 5G NR standard signals in perceptive mobile networks by applying one-dimension (1D) to 3D CS algorithms.
- We propose a cluster based Kronecker OMP algorithm that exploits the cluster structure in multipath channels for more accurate sensing parameter estimation in perceptive mobile networks.

This rest of the paper is divided into four parts. The first part provides 5G usable signal and channel description. The second part describes various sensing parameter estimation algorithms including 1D, 2D, and 3D in detail. In the third part, we illustrate our proposed 2D cluster Kronecker CS algorithm. Finally, in the fourth part, we discuss simulation results and outline a comparative study from these results obtained from 5G reference signals.

II. Signal and Channel Models

We consider 5G-compatible signals with OFDMA and SDMA (or multi-user MIMO) modulations. In a typical setup, there are 4 SDMA users, each with a single antenna, and a BS with a 16 antenna uniform linear array. The signal bandwidth is assumed to be 100 MHz.

DMRS is used as a primary signal for sensing. Propagation channels are generated based on clustered channel models of two forms. The first one is developed by us and named as *Cluster-Chl* [2], and the second one is the *QuaDRiGa* channel model [27], recommended by 3GPP for modelling communication channels in LTE and 5G systems.

A. DMRS Signal Generation

DMRS signal is generated according to the Gold sequence as defined in [21] of *3GPP TS 38.211*, both for *Physical Downlink Shared Channel-PDSCH* and *Physical Uplink Shared Channel-PUSCH*. The generated physical resource-block (PRB) indicates DMRS to a 3-D grid comprising a 14-symbol slot for the full carriers across the DMRS layers or ports. The values and indices of DMRS signals are both known to the BS, and are used as prior when doing sensing from received signals. Here, interleaved DMRS subcarriers of PDSCH are used in downlink sensing, while groups of non-interleaved DMRS subcarriers of PUSCH are used in uplink sensing.

B. Channel Modelling

For radio sensing, the system needs to interpret detailed channel structure and estimate the sensing parameters. Our used propagation channels are generated based on clustered channel models following the 3GPP channel models for LTE and 5G systems [21]. Random and continuous values are used for delay, Doppler shift, angle-of-arrivals (AoAs) and angle-of-departures (AoDs) as actual *sensing parameters* to be estimated. The multipaths of the channels are generated in clusters, indicating reflections coming from scattering obstacles. That is, each cluster of paths, which come from a single or multiple closely located scatter obstacles, have close values of sensing parameters. We generate approximate scatters for simulating sensing by using both the Cluster-Chl and QuaDRiGa model.

Let N denote the number of total subcarriers and B the total bandwidth. Then the subcarrier interval is $f_0 = B/N$ and OFDM symbol period is $T_s = N/B + T_p$ where T_p is the period of cyclic prefix.

Consider a narrowband antenna array model . The array response vector of a size-M array with θ of either AoD or AoA is,

$$\mathbf{a}(M,\theta) = [1, e^{j\pi\sin(\theta)}, \cdots, e^{j\pi(M-1)\sin(\theta)}]^H, \quad (1)$$

For M_1 transmitting and M_2 receiving antennas, the $M_2 \times M_1$ time-domain baseband channel impulse response (CIR) matrix at time t' can be represented as

$$\tilde{\mathbf{H}}(t') = \sum_{\ell=1}^{L} b_\ell \delta(t'-\tau_\ell) e^{j2\pi f_{D,\ell} t'} \mathbf{a}(M_2,\phi_\ell)\mathbf{a}^T(M_1,\theta_\ell), \quad (2)$$

where for the ℓ-th out of a total of L multipath signals, θ_ℓ and ϕ_ℓ denote the AoD and AoA, respectively, b_ℓ, τ_ℓ and $f_{D,\ell}$ are the amplitude, propagation delay, and Doppler frequency, respectively.

1) Cluster-Chl Channel Model: In Cluster-Chl, we have a flexible control on all the channel parameters. The multipath channels of Cluster-Chl are randomly generated in clusters following a complex Gaussian distribution to generate sensing parameters for moving objects around the mobile network node, which mimics the ray tracing model and are extensions of the Saleh-Valenzuela (S-V) model [28].

In Cluster-Chl, we generate 3 clusters with delay centered at 29, 39 and 49 μs, corresponding to a distance of 87, 117 and 147 meters, with AoA center randomly generated between -120 to 120 degrees, and moving speed randomly generated between 0 to 40 m/s. In each cluster, as like we did in [3], [4], multipath signals for each RRU/MS are generated randomly by mimicking reflected/scattered signals from objects. In each cluster, the multipath is generated following a uniform distribution of [5, 10] for the total number, [0, 28] degrees for direction span, [0, 0.05] μs for delay (corresponding to [0, 15] m for distance). We use a pathloss model with pathloss factor 40 for downlink and 20 for uplink sensing. The transmission power of the RRU and MS is 30 dBm and 25 dBm respectively. The total thermal noise in the receiver is $-174 + 10\log(10^8) = -94$ dBm.

2) QuaDRiGa Channel Simulator: QuaDRiGa is a spatial geometry based 3D MIMO channel generator [27], originated from the *WINNER* series models and supports rich cluster multipath scenarios specified by the 3GPP-3D cluster-based models mentioned in *TR 36.873 and TR36.901* [27]. We generate QuaDRiGa channels equivalent to moving scatters by simulating moving transmitters and receivers from open source simulator for sensing demonstration. Non-line of sight channels are simulated. One problem with the QuaDRiGa model is that scatters can not be accurately placed and configured. The other problem is that the Doppler frequencies for each multipath is not explicitly provided and hence we cannot verify the accuracy of estimates.

C. Received Signal Model for Sensing

The received radar signal data is based on 3D observation samples, comprising of those from multiple receiving antennas, multiple DMRS subcarriers and multiple DMRS signals over time. The modulated data symbols can be removed from the received DMRS signals by applying equalization, which will be a simple one-tap multiplication if no two users are sharing the same subcarrier. In this paper, we consider the case that only each subcarrier is used by only one user in DMRS signals. In this case, the signals for different users are orthogonal in the frequency domain and hence no multi-user interference (MUI) exists. After the equalization, the processed received signal at the n-th subcarrier and the t-th DMRS signal can be represented as

$$\mathbf{Y}_{n,t} = \sum_{\ell=1}^{L} b_\ell e^{-j2\pi n\tau_\ell f_0} e^{j2\pi t f_{D,\ell} T_s} \cdot \mathbf{a}(M_2,\phi_\ell)\mathbf{a}^T(M_1,\theta_\ell) + \mathbf{z}_{n,t}, \quad (3)$$

$$= \mathbf{A}_{rx}\mathbf{C}_n\mathbf{D}_t\mathbf{A}_{tx}^T + \mathbf{z}_{n,t}, \quad (4)$$

where the ℓ-th column in $\mathbf{A}_{rx}$ and $\mathbf{A}_{tx}^T$ are $\mathbf{a}(M_2,\phi_\ell)$ and $\mathbf{a}^T(M_1,\theta_\ell)$, respectively; if there is no two multipath having the same delay values, $\mathbf{D}_t$ and $\mathbf{C}_n$ are diagonal matrices with the ℓ-th diagonal element being $b_\ell e^{j2\pi t f_{D,\ell} T_s}$ and $e^{-j2\pi n\tau_\ell f_0}$, respectively, otherwise there will be non-zero values in other entries; and $\mathbf{Z}_{n,t}$ is the noise matrix. When each user only has one transmitting antenna, $\mathbf{A}_{tx}^T$ becomes a all-one column vector, and $\mathbf{Y}_{n,t}$ and $\mathbf{Z}_{n,t}$ become column vectors too. The task for sensing parameter estimation is to estimate $\{\tau_\ell, f_{D,\ell}, \phi_\ell, \theta_\ell, b_\ell\}, \ell \in [1, L]$ from the received signals.

III. CS-based Sensing Parameter Estimation

Our developed and tested 1D, 2D and 3D CS algorithms for sensing parameters estimation are extended from the 1D-CS algorithms [29], 2D Kronecker CS [30], and 3D N-way Tensor tool [31], respectively. The extensions formulation and processing are realized here through extracting sensing parameters from 5G received signals. We test these algorithms utilizing Cluster-Chl in downlink sensing and the QuaDRiGa model in uplink sensing. We also compare our 1D to 3D results with the cases when the occupied PRB is small in uplink and with the results from 2D discrete Fourier transform (DFT).

Since the signals are relatively independent in the three domains of delay, AoA and Doppler, they can be formulated in a high-dimension (3D here) vector Kronecker product form. Therefore, we can apply 1D to 3D CS techniques to estimate these sensing parameters. In a typical system, we can get a sufficient number of observations for the delay (linked to the number of subcarriers), intermediate AoA observations (linked to the number of antennas) and a limited number of samples in the Doppler domain (linked to DMRS signals over a portion of channel coherent period). The Doppler frequency is typically very small in a perceptive mobile network and the accumulated phase shift usable is also small due to the limited period of channel coherent time. This makes it inaccurate for estimating Doppler using CS algorithms. Next, we briefly review each of the three sensing algorithms based on the received signal in (4).

A. 1D Compressive Sensing

We assume that there is only one multipath signal within each quantized delay bin for each cluster in the 1D CS based algorithm. By stacking the signals in (4) from all available subcarriers to one matrix, we can get

$$\mathbf{Y}_t = \mathbf{W}\underbrace{\mathbf{D}_t\mathbf{A}_{rx}^T}_{\mathbf{G}_t} + \mathbf{Z}_t, \quad (5)$$

where the ℓ-th column of $\mathbf{W}$ is $\{e^{-j2\pi n\tau_\ell f_0}\}$. We can then treat (5) as an on-grid multi-measurement vector (MMV) CS

problem and use algorithms such as 1D sparse Bayesian CS to get the estimate for $\mathbf{G}_t$. The dictionary $\mathbf{\Psi}_1$ is a partial DFT delay matrix, approximating $\mathbf{W}$. Once the delays and $\mathbf{G}_t$ are estimated, we can get the AoA estimates through calculating the cross-correlation between columns from $\mathbf{G}_t$ on the indexes obtained from given threshold as below,

$$\hat{\phi}_\ell \approx \frac{1}{\pi}\angle\left(\sum_{p=1}^{M-1}((\mathbf{G}_t)_{\cdot,p})^*(\mathbf{G}_t)_{\cdot,p+1}\right), \tag{6}$$

where $(\mathbf{G}_t)_{\cdot,p}$ denote the p-th column $\mathbf{G}_t$. The Doppler frequency $f_{D,\ell}$ can be estimated across multiple DMRS signals, based on the cross-correlation of $(\mathbf{G}_t)_{\ell,\cdot}$, where $(\mathbf{G}_t)_{\ell,\cdot}$ denotes the ℓ-th row of $\mathbf{G}_t$. Assume the interval between every two estimates of $\mathbf{G}_t$ and $\mathbf{G}_{t+1}$ is uniform and be T_s for any t, which can be relaxed easily. Let N_d be the total OFDM blocks used for estimating the Doppler frequency. Then,

$$\hat{f}_{D,\ell} \approx \frac{1}{2\pi T_s}\angle\left(\sum_{t=1}^{N_d-1}((\mathbf{G}_t)_{\ell,\cdot})((\mathbf{G}_{t+1})_{\ell,\cdot})^*\right). \tag{7}$$

The main advantage of the 1D algorithm is that it can accurately estimate all the parameters when each multipath is well separated in delay. Its complexity is also relatively low. It is mostly suitable for systems with a large number of subcarriers, but small number of antennas for AoA estimation and packets for Doppler estimation.

B. 2D Kronecker Compressive Sensing

2D Kronecker CS can obtain direct estimation for any two parameters out of delay, AoA and Doppler. Since we can have sufficient measurements in the delay and AoA domain, the 2D CS algorithm can provide good estimates for both delay and AoA directly from $\mathbf{Y}_t$ of (5) using each DMRS signal of 2D observations. We construct two dictionaries for delay and AoA, $\mathbf{\Psi}_1$ and $\mathbf{\Psi}_2$, being two partial overcomplete DFT matrices, approximating $\mathbf{W}$ and $\mathbf{A}_{rx}$, respectively. Let N_1 and N_2 be the number of codes, i.e., the number of columns, in $\mathbf{\Psi}_1$ and $\mathbf{\Psi}_2$. Interpolated overcomplete dictionaries are used to improve resolution at an increased computational complexity, given that the signal to noise power ratio (SNR) is sufficiently large. We can then obtain estimates $\hat{\mathbf{D}}_t$ of size $N_1 \times N_2$ for the expanded matrix for $\mathbf{D}_t$ that corresponds to the two overcomplete dictionaries, using any 2D Kronecker CS algorithm, such as the 2D-OMP algorithm [30].

Note that the 2D CS algorithm here can identify any pair of {delay, AoA} with at least one different value. So $\hat{\mathbf{D}}_t$ will not be a diagonal matrix anymore if one variable in the pair has two identical quantized values. After getting the estimate $\hat{\mathbf{D}}_t$, we use a threshold to filter out very small estimates which are likely caused by noise. We can then get the delay and AoA estimates according to the indexes of the non-zero values in $\hat{\mathbf{D}}_t$, corresponding to respective columns in the two dictionaries $\mathbf{\Psi}_1$ and $\mathbf{\Psi}_2$.

The Doppler shift is estimated via calculating the angle of the cross-correlation values between the non-zero values of $\hat{\mathbf{D}}_t$ obtained over two DMRS signals. This represented as

$$\hat{f}_{D,\ell} \approx \frac{1}{2\pi T_s}\angle\left(\hat{\mathbf{D}}_t\hat{\mathbf{D}}_{t+1}^*\right)_{\ell,\ell}. \tag{8}$$

Averaging can be taken over the correlation obtained from multiple DMRSs before computing the angle, to improve the accuracy of the estimates.

2D CS algorithm can achieve improved estimation accuracy when there are multipath with repeated values in any one domain, at the cost of increased complexity.

C. 3D Tensor Compressive Sensing

The Tensor-OMP CS algorithm directly estimates parameters in a 3D domain, combining measurements $\mathbf{Y}_t$ over multiple DMRS signals. Three dictionaries, $\mathbf{\Psi}_1$, $\mathbf{\Psi}_2$, and Doppler dictionary matrix, $\mathbf{\Psi}_3$, are utilized. Since the accumulated Doppler shift is small over the coherent time period, we have to use a portion of highly overcomplete DFT matrix as $\mathbf{\Psi}_3$.

Absolute values of the estimated sparse coefficients provide the amplitude values of multipaths. After applying a threshold, each of indexes in the three dimensions corresponding to non-zero estimates provides estimated values for τ_ℓ, ϕ_ℓ, and $f_{D,\ell}$.

Generally, high-order CS formulation using Tensor tools such as 3D Tensor CS provides the strongest estimation performance in resolving multipath with repeated parameter values. However, it involves much higher computational complexity than 2D and 1D, using three dictionaries $\mathbf{\Psi}_1$, $\mathbf{\Psi}_2$, and $\mathbf{\Psi}_3$, in direct estimation of parameters in 3D domain from $\mathbf{Y}_t$. In addition, as the Doppler shift value is small, 3D will not work as well as 1D and 2D.

IV. Cluster-based Sensing Parameter Estimation

In our earlier proposed JCAS solutions, for example, in [3], in [4] and in Section III we cast the radio sensing problem as a block sparse/sparse reconstruction problem. However, in practice, multipath signals always arrive in clusters [28], and paths from one cluster typically come from the same scatter(s) and have close parameter values.

Referring to the 5G NR standard signals and channel described in section II, we use the OFDM-type DMRS 5G usable signals and Cluster-Chl channel [2] for sensing using the proposed algorithm based on 2D Kronecker (kron) orthogonal matching pursuit (OMP) techniques. We consider both downlink and uplink sensing, where downlink and uplink communication signals are used for sensing, respectively.

A. 2D Cluster Kron-OMP Algorithm

Since the signals are relatively independent in the three domains of delay, AoA and Doppler, they can be formulated as a 3D cluster sparse signal. Then, we can apply cluster based greedy method equipped with cluster prior probability to estimate these sensing parameters. In a typical system, we can get a sufficient number of observations for the delay (linked to the number of subcarriers), AoA (linked to the number of antennas) and a limited number of samples in the Doppler domain (linked to DMRS signals over a portion of channel coherent period).

We assume that there is only one multipath signal within each quantized delay bin. Let M_r and M_T denote the number of antennas for receiving in BS and in each user for

transmitting, respectively. Let $\mathscr{S}_s$ denote the set of available subcarriers for sensing and let N_s denote its size. Referring to (4), after stacking signals $\mathbf{Y}_{n,t}, n \in \mathsf{S}$ from all available subcarriers to a matrix and we obtain

$$\mathbf{Y}_t = \mathbf{W} \underbrace{\mathbf{D}_t \mathbf{A}_{tx}}_{\mathbf{G}_t} \mathbf{A}_{rx}^T + \mathbf{Z}_t, \tag{9}$$

where $\mathbf{W}$ is a $N_s \times L$ matrix with its ℓ-th column being $\{e^{-j2\pi n \tau_\ell f_0}\}$. Note that N_s is typically smaller than N and the indexes of subcarriers are often dis-continuous.

We construct two dictionaries for AoA and delay, $\mathbf{\Psi}_1$ and $\mathbf{\Psi}_2$, being two partial overcomplete DFT matrices, approximating $\mathbf{A}_{rx}$ and $\mathbf{W}$, respectively. Let N_A and N_D be the number of codes, i.e., the number of columns, in $\mathbf{\Psi}_1$ and $\mathbf{\Psi}_2$. In practical applications, the non-zero entries of the sparse signals appear in clusters over each column of the matrix $\mathbf{G}_t$ in $\mathbf{Y}_t$. We can then treat (9) as an on-grid 2D cluster sparse CS problem with a $M_r \times N_s$ observation matrix $\mathbf{Y}_t$, two dictionaries $\mathbf{\Psi}_1$ and $\mathbf{\Psi}_2$, and block sparse signals $\mathbf{G}_t$ of k- sparsity that appears in clusters. Such a problem can be solved by using, e.g., the 2D block sparse Bayesian CS in and 2D kron-OMP in . However, no prior information on the cluster structure is properly applied in these CS solutions.

Our proposed novel 2D cluster kron-OMP algorithm incorporates a cluster prior Δ to the sparse probability of each entry in the support set, ξ. Such an incorporation exploits both cluster structure and sparsity in the solution than conventional 2D kron-OMP algorithms.

For producing the cluster prior Δ, at each iteration, inspired from the neighborhood model [32], we can compute the cluster pattern through measuring the changes in the values of ξ. We first compute the absolute sum of the differences in the support set ξ via

$$\Delta(\xi) = \sum_{i=1}^{k} |\, \xi_i - \xi_{i-1} |\,. \tag{10}$$

The cluster prior for the support learning vector ξ is dependent on the term $e^{-\alpha(\Delta(\xi))}$ for $\alpha > 0$. Since the entries of the sensing parameters and noise component are drawn from Gaussian distribution, we need to employ a distribution which is conjugate to the Gaussian distribution, for example, a Gamma distribution, to promote the cluster pattern with the sparse prior [33], [34]. Hence, we model the behavior of the function $e^{-\alpha(\Delta(\xi))}$ via the Gamma distribution as,

$$(\Delta|\beta, \alpha) \sim \Gamma(\beta, \alpha), \tag{11}$$

where β and α are the shape and rate parameters of the Gamma distribution, respectively. We also assume that $\beta = 1$ and as a result,

$$(\Delta|\beta, \alpha) \propto e^{-\alpha\Delta}. \tag{12}$$

The conditional joint probability density function of $\mathbf{Y}_t$ and Δ can be written as

$$\begin{aligned} &P(\mathbf{Y}_t, \Delta|\alpha, \mathbf{\Psi}_1, \mathbf{\Psi}_2, \mathbf{G}_t, \xi) \sim \\ &P(\mathbf{Y}_t|\mathbf{\Psi}_1, \mathbf{\Psi}_2, \mathbf{G}_t, \xi, \alpha, \Delta) P(\Delta|\beta, \alpha). \end{aligned} \tag{13}$$

Algorithm 1: 2D Cluster Kron-OMP Algorithm

Require: Estimation of $\boldsymbol{G}_t$.

Input: Observation matrix $\mathbf{Y}_t \in \mathbb{R}^{M_r \times N_s}$, combined dictionary $\mathbf{\Psi} = (\mathbf{\Psi}_1 \in \mathbb{R}^{M_r \times N_A}, \mathbf{\Psi}_2 \in \mathbb{R}^{N_s \times N_D})$, iteration control threshold ρ, sparsity k, initial cluster sparse estimate $\hat{\mathbf{G}}_t = \emptyset$, initial index $J_0 = \emptyset$

Output: Reconstructed signal $\hat{\mathbf{G}}_t$ after k iteration, non-zero positions J, residual $\boldsymbol{R}^{(k)}$

1: **Initialization** $\boldsymbol{R}^{(0)} = \mathbf{Y}_t$
2: **while** $i \leq k$ **do**
3: Compute $\mathbf{\Xi} = \mathbf{\Psi} * \boldsymbol{R}^{(i)}$
4: Compute index J so that $\max \left|\mathbf{\Xi}^i\right|$ {finding the atom and indexes J in cases where $\mathbf{\Psi}$ is with maximum correlation with residual}
5: Compute Δ
6: Update ξ with extracted J now at with probability proportional to $\max \left|e^{((c^2/2(\sigma)^2 * \mathbf{\Xi}^i) - \alpha\Delta)}\right|$ and update the support ξ as $\xi^i = \xi^{i-1} \cup J$
7: Update α from $\Gamma(\eta, \theta + \Delta)$
8: Compute $\mathbf{\Omega} = \text{pinv}(\mathbf{\Psi}_2{}^* \bigotimes \mathbf{\Psi}_1)\mathbf{Y}_t$
9: Update $\boldsymbol{R}^{(i)} = \mathbf{Y}_t - \mathbf{\Psi}_1 \text{diag}(\mathbf{\Omega}) \mathbf{\Psi}_2{}'$
10: If $\boldsymbol{R}^{(i)} < \rho$, $i = i + 1$
11: Compute $\hat{\mathbf{G}}_t = \text{sptensor}(J_i, \mathbf{\Omega}, M_r)$
12: **end while**

With the constructed prior probabilities, we can then extend conventional 2D kron-OMP algorithms to incorporate such prior information. The proposed 2D cluster kron-OMP algorithm is detailed in Algorithm 1.

Initially at iteration $i = 0$, the residual value $\boldsymbol{R}^{(0)}$ is set as $\mathbf{Y}_t$ and the initial non-zero index locations are set as $J_0 = \emptyset$. As the iteration progresses, we find the updated indexes J at step 4 by $\max \left|\mathbf{\Xi}^{\boldsymbol{i}}\right|$, corresponding to the case where the dictionary $\mathbf{\Psi}$ has maximum correlation with the residual $\boldsymbol{R}^{(i)}$. After computing Δ in step 5, the support set ξ is updated at step 6 with the extracted index locations J by utilizing the joint probability density function in (13). The prior on the parameter α in (11) is assumed to have Gamma distribution, $\alpha|\eta, \theta \sim \Gamma(\eta, \theta)$, and we experimentally set $\eta = \epsilon$ and $\theta = 1$, where ϵ denotes the length of the support learning vector ξ. With the progression of measurements, at step 7, the posterior density on α is updated. This posterior distribution can be described as,

$$P(\alpha|\eta, \theta, \Delta) \sim \Gamma(\eta, \theta + \Delta), \tag{14}$$

where $P(\alpha|\eta, \theta, \Delta)$ denotes the conditional posterior density on α given the related parameters. We estimate this via $E[\alpha|\eta, \theta, \Delta] = \eta/(\theta + \Delta)$. Then, we compute $\mathbf{\Omega}$ as the multiplication product of $\mathbf{Y}_t$ and Moore-Penrose pseudoinverse of kronecker product of $\mathbf{\Psi}_1$ and $\mathbf{\Psi}_2$ in step 8. Finally the estimate $\hat{\mathbf{G}}_t$ is computed as a sparse matrix of size $N_A \times N_D$ derived from open MATLAB sparse tensor (sptensor) toolbox [35] with J_i and $\mathbf{\Omega}$ for M_r. The algorithm usually stops when the iteration i reaches the desire sparsity level of k for $\hat{\mathbf{G}}_t$.

B. Estimation of Sensing Parameters

The proposed 2D cluster kron-OMP algorithm can obtain direct estimation for any two parameters out of delay, AoA and Doppler. Since we can have sufficient measurements in the delay and AoA domain, the algorithm can provide good estimates for both delay and AoA directly from $\mathbf{Y}_t$ of (5) using each DMRS signal of 2D observations. Note, in step 6 of Algorithm 1, $c = 1/(1+\sigma^2)$, where σ^2 is the thermal noise variance. We can obtain efficient estimates $\hat{\mathbf{G}}_t$ and non-zero indexes J for the expanded matrix of $\mathbf{G}_t$ that corresponds to $\mathbf{\Psi}$, using the prior cluster structure knowledge.

Note that the proposed algorithm can identify any pair of {delay, AoA} with at least one different value. So $\hat{\mathbf{G}}_t$ will not be a diagonal matrix anymore if one variable in the pair has two identical quantized values.

After getting the estimate $\hat{\mathbf{G}}_t$, we can then get the delay and AoA estimates according to the J indexes of the non-zero values in $\hat{\mathbf{G}}_t$, corresponding to respective columns in the two dictionaries.

The Doppler shift is estimated via calculating the angle of the cross-correlation values between the non-zero values of $\hat{\mathbf{G}}_t$ obtained at J indexes over two DMRS signals. Assume the interval between every two estimates of $\mathbf{G}_t$ and $\mathbf{G}_{t+1}$ is uniform and be T_s for any t, which can be relaxed easily. This can be represented as

$$\hat{f}_{D,\ell} \approx \frac{1}{2\pi T_s} \angle \left(\hat{\mathbf{G}}_t \hat{\mathbf{G}}^*_{t+1} \right)_{\ell,\ell}. \tag{15}$$

Averaging can be taken over the correlation obtained from multiple DMRSs before computing the angle, to improve the accuracy of the estimates.

V. Simulation Results

A. 1D-3D Sensing Results

Next, we present simulation results for 1D to 3D CS using channels with continuous-value (off-grid) sensing parameters. We also show the results obtained by directly applying 2D-DFT over delay-AoA and delay-Doppler domains for comparison, when all subcarriers are used. Of course, most of the time, not all subcarriers are available for sensing. Estimated values (typically shown in blue star) are placed with actual ones (shown in red circle) to verify the accuracy of estimation. Fig. 2 shows an exemplified CIR for QuaDRiGa channels consisting of rich multipaths with 4 to 5 clusters where "Equivalent AOA" equals to $\pi \sin(\phi)$.

1) Downlink Sensing : In downlink sensing, we use DMRS subcarrier configuration type-1 slot wise, with every alternating subcarrier as an interleaved selection from a total of 252 subcarriers. Sub-interval is 2 for type-1, so, in total 126 subcarrier indices (e.g. of layer 4) are used as DMRS subcarriers.

The simulation results for downlink sensing with Cluster-Chl model are presented in Fig. 3 for 1D to 3D. For 1-D CS, AoA-Distance and Speed-Distance result indicates that the estimated points are well matched with three clusters with few extra points due to residual in threshold setting. Off-grid estimation causes some missed detection. In 2D CS, AoA-Distance and Speed-Distance results give few mismatched

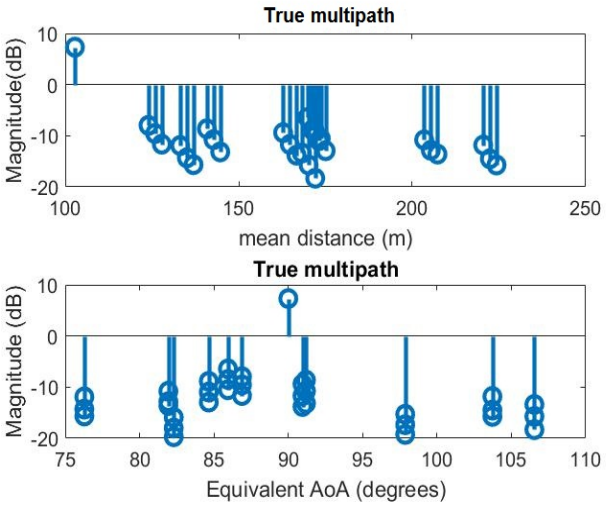

Fig. 2: CIR for QuaGRiGa channel

points for both AoA and speed. In 2D, there is an important observation that interleaved subcarriers in this case actually cause ambiguity in estimation. 3D estimation results are not as good as 1D and 2D CS algorithms as in 3D estimation the interleaved subcarriers cause near-singular matrix.

The ambiguity is caused by non-consecutive, but regularly spaced samples, for example, usage of comb or interleaved subcarriers [36]. In this case, the actual value can be one of the multiple integral times of a basic estimate. The simplest way is to break such regularly spaced samples, for example, we can randomly select samples from the total available ones such that the indexes of these samples are not regular. This, of course, reduces the samples used for estimation and may degrade the estimation performance particularly when the number of samples is small. Therefore, while using DMRS, alternative methods can be based on exploiting other information to assist the selection of the right estimate, for example, the magnitude, or an integration of coarse and fine estimation methods. This is, in fact, one of our future work on how to solve ambiguity that may be present in all domains, but particularly for the delay.

2) Uplink Sensing : In uplink sensing, only partial DMRS subcarriers are used. The details of obtained results from the non-line-of-sight (NLOS) QuaDRiGa channel model are given here. We use DMRS subcarrier configuration type-2 non-slot wise, which indicates several groups of subcarriers are selected from a total of 252 subcarriers. Sub-interval is 3 for type-2, so, in total 84 subcarrier indices (of layer 4) are used as DMRS subcarriers. We use QuaDRiGa model where clusters are generated with continuous delay and AoA values for multipaths. Since the QuaDRiGa model unable to provide actual Doppler shifts, the estimates given here in all uplink sensing for speed are relative only.

3) Uplink Sensing with QuaDRiGa NLOS: Fig. 4 provides simulation results for uplink sensing with QuaDRiGa NLOS for 1D to 3D. In 1-D CS, AoA-distance results for the estimated points fairly match with several clusters with few extra points due to residual in threshold setting and off-grid

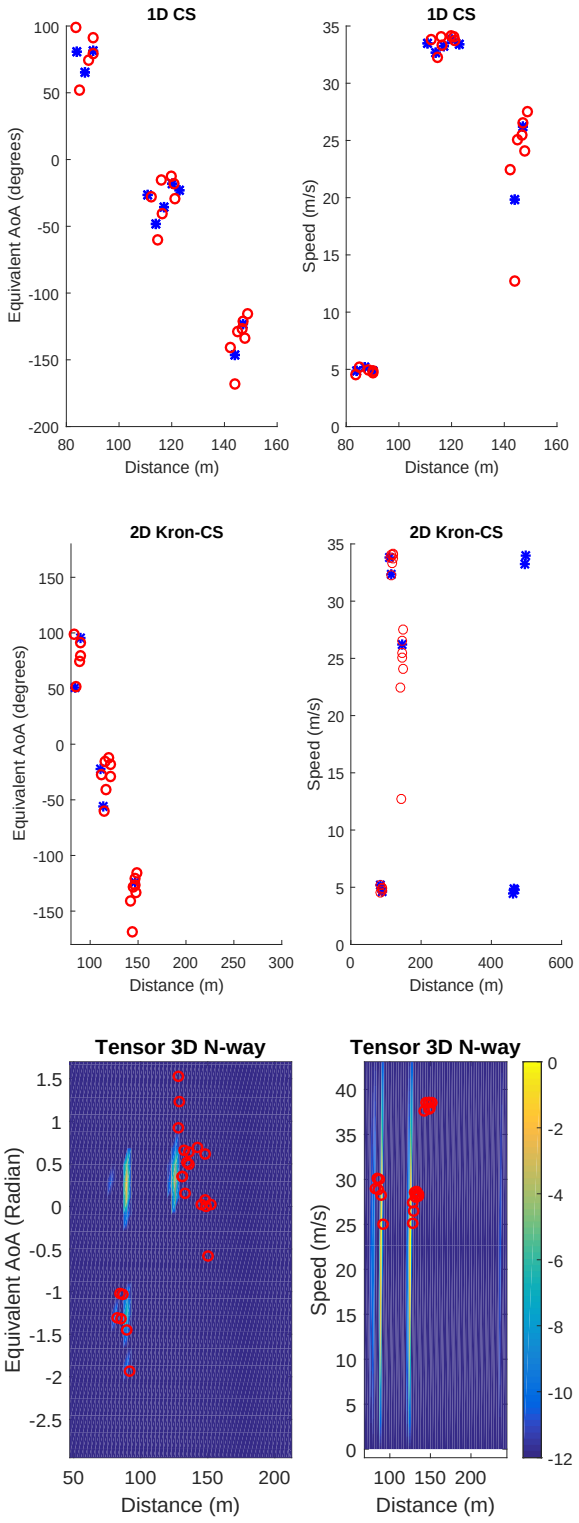

Fig. 3: Observations in Cluster-Chl for downlink sensing

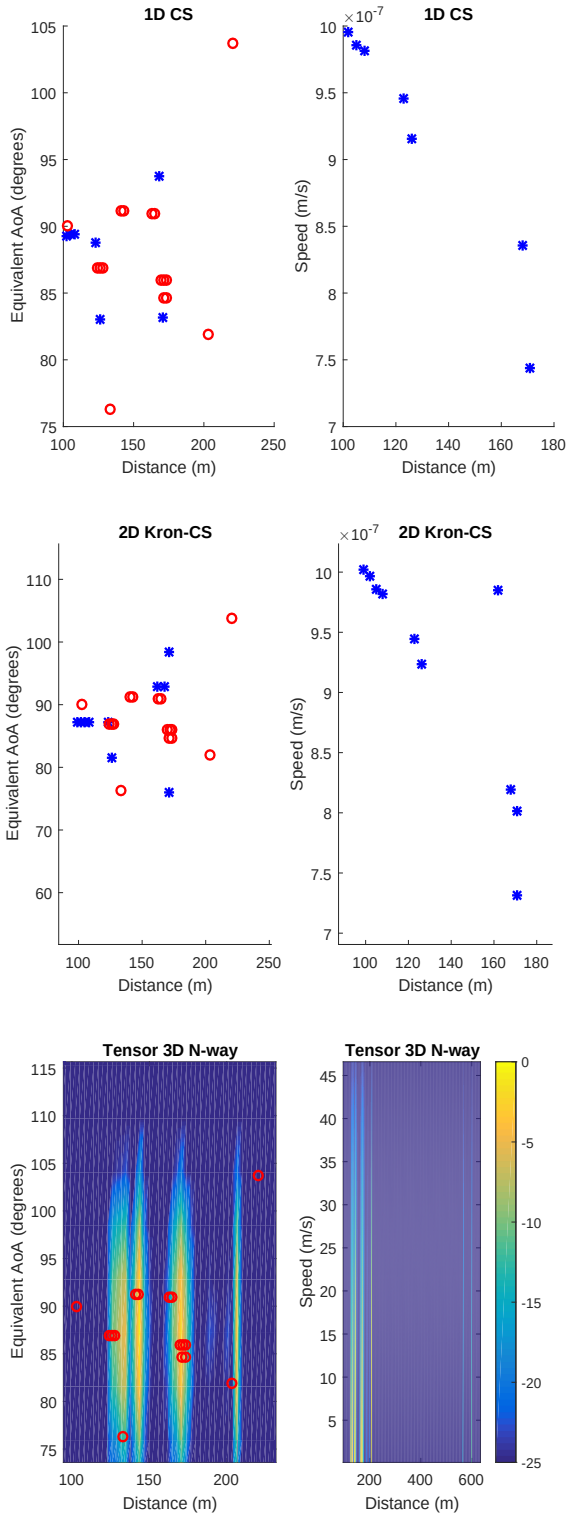

Fig. 4: Observations in uplink sensing: QuaDRiGa NLOS

error.

2D CS AOA-distance results indicate that estimated values are in closer vicinity with actual clustered multipath values (AoA) in comparison with 1D. Indeed, a higher dimensional sensing algorithm like the 2D kron CS eventually provides better performance when there are enough measurements because it can directly identify two parameters only if one is different between any multipath channels. In both figures for 3D Tensor OMP, only estimated multipath channels with power within -15 dB of the maximum are shown. In 3D, estimated values for AoA are coarser, but remain within the close neighbouring of actual values.

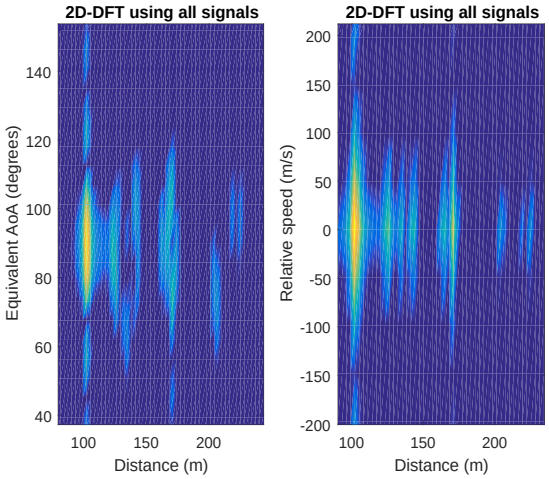

Fig. 5: 2-D DFT for uplink sensing

4) 2D DFT results for uplink Sensing: 2D-DFT simulation results are presented in Fig. 5 for QuaDRiGa channels. It can be observed that 2D-DFT provides reliable coarse estimates for uplink sensing, but the resolution is very low in comparison with all results of 1D to 3D in Fig. 4. It is noted that here the results are obtained by using all subcarriers. Such a 2D-DFT method only works when either all or interleaved subcarriers are available.

5) Sensing Using Limited Number of PRBs: Mainly in the uplink direction, allocated PRB could be limited by configuration [21]. Therefore, we can only get small amount of observations for the delay estimation, which could be even less than the number of multipath. We test sensing with such a limited number of resources for QuaDRiGa NLOS channel here. Assume that only 28 DMRS subcarriers (7 PRB) are used in simulations for uplink sensing. Fig. 6 presents uplink sensing for 7 PRBs with QuaDRiGa NLOS for 1D to 3D. In 1D CS, the resolution ambiguity problem remains in the delay domain. However, the shape still well maintained. Reasonable estimation accuracy is found in AoA by 2D. Coarse estimation in both AoA and speed is obtained by 3D. Further approaches to increasing this accuracy in radio sensing from limited observations, especially in the clustered multipath environment will be studied in our future research, for example, by designing better dictionaries and using filtering techniques.

B. 2D Cluster Kron CS Results

In this section, we present simulation results for direct estimation over delay-AoA and delay-Doppler domains using quantized and continuous-value sensing parameters. Estimated values (typically shown in blue star) are placed with actual ones (shown in red circle) to verify the accuracy of estimation.

Fig. 7 shows an exemplified CIR for 3-cluster Cluster-Chl channel consisting of rich multipaths. Propagation paths in each cluster have close parameter values particularly in the distance (delay) domain, and different clusters are distinguished by different colors.

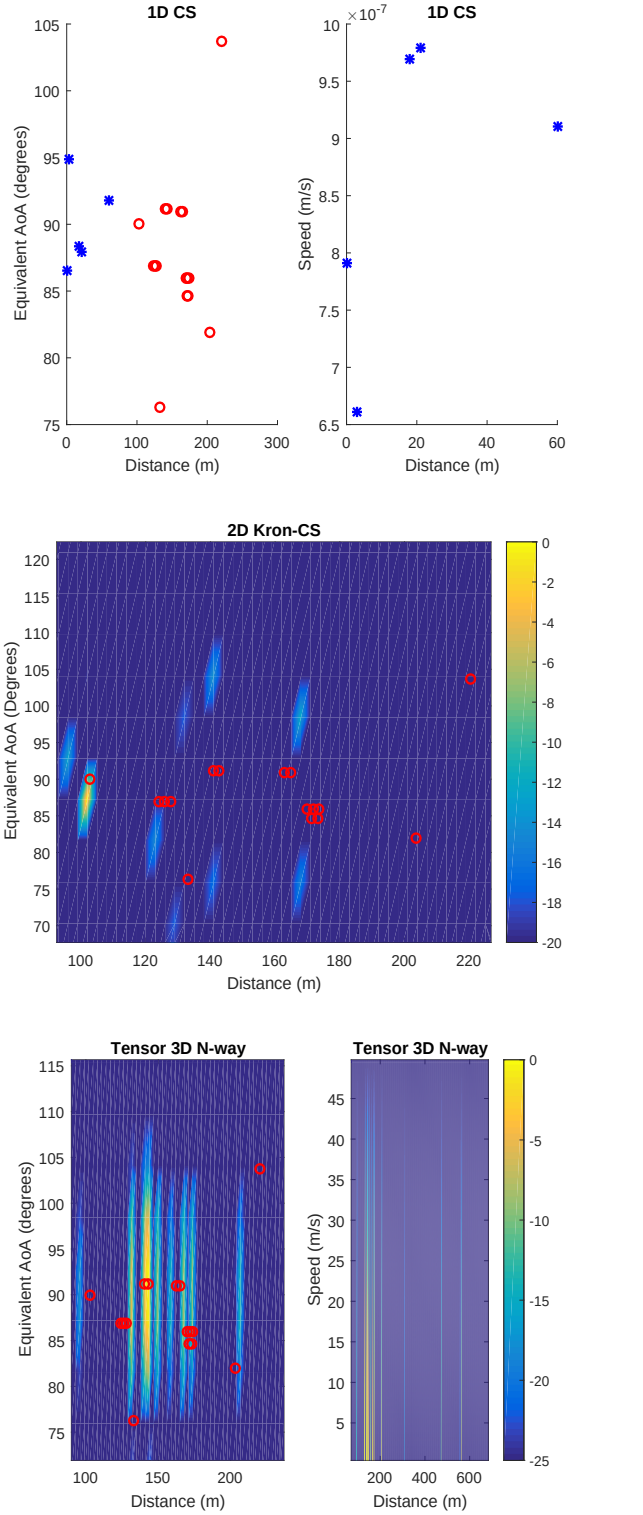

Fig. 6: Uplink sensing with 7 PRBs in QuaDRiGa NLOS

1) Downlink Sensing: In downlink sensing, we use DMRS subcarrier configuration type-1 slot-wise, with every alternating subcarrier selected from a total of $N = 252$ subcarriers. So, in total $N_s = 126$ DMRS subcarriers are used. Total 8 OFDM samples or packets used for estimating the Doppler frequency.

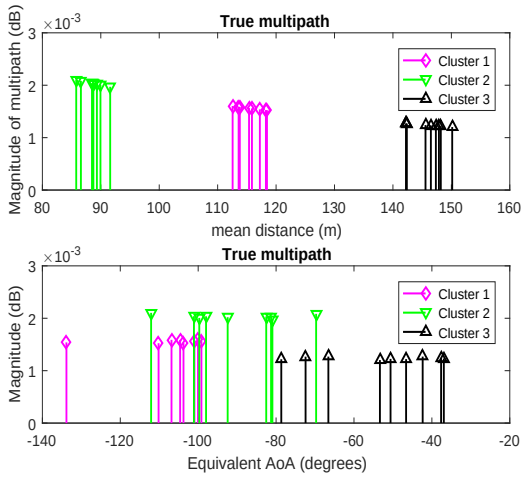

Fig. 7: CIR for cluster channel

The simulation results are presented in Fig. 8 for the case when the proposed 2D cluster kron-OMP algorithm is applied to delay-AoA and delay-Doppler domains, respectively. For quantized on-grid parameters, as shown in the top two sub-figures, we can obtain a nearly perfect estimation of delay, AoA and Doppler. For continuous off-grid parameters, as shown in the bottom two sub-figures, performance degradation can be observed with reduced accuracy and missed estimates. However, the estimates preserve the cluster structure and convey correct information for determining the location and moving speed of the scatters.

2) Uplink sensing : For uplink sensing, the allocated PRB (subcarriers) is limited by configuration and we have fewer subcarriers available. The results, in this case, can particularly show the usefulness of the proposed algorithm. In the simulation, channel clusters are generated with continuous delay and AoA values. For DMRS subcarriers, we take the configuration of type-2 with non-slot-wise subcarrier, where only $N_s = 28$ DMRS subcarriers (7 PRB) of layer 4 are used.

Fig. 9 provides the simulation results for the proposed algorithm. Both AoA-distance and Speed-Distance results for the estimated points are well matched with all clusters. However, there are a few missed estimates for speed.

For comparison, we present the simulation results in Fig. 10 for the conventional 2D kron-OMP method [30] that does not consider cluster prior so that we can directly compare the actual accuracy of estimates obtained in Fig. 9. There are some major problems with this method, compared to the proposed one. Firstly, we note that there exists the estimation accuracy problem and hence missed estimation occurs in cluster channels, which is overcome by the cluster prior in the proposed algorithm. Secondly, we have to use a threshold of $T_h = -15\ dB$ to pick up "effective" estimates with significant power. Comparatively, in the proposed algorithm, the indexes are generated automatically without using any explicit threshold. Thirdly, even when we relax the accuracy requirement of the estimates and observe the zoomed box section of estimates, we can see that the estimates are hardly following the cluster pattern of the actual ones in Fig. 10.

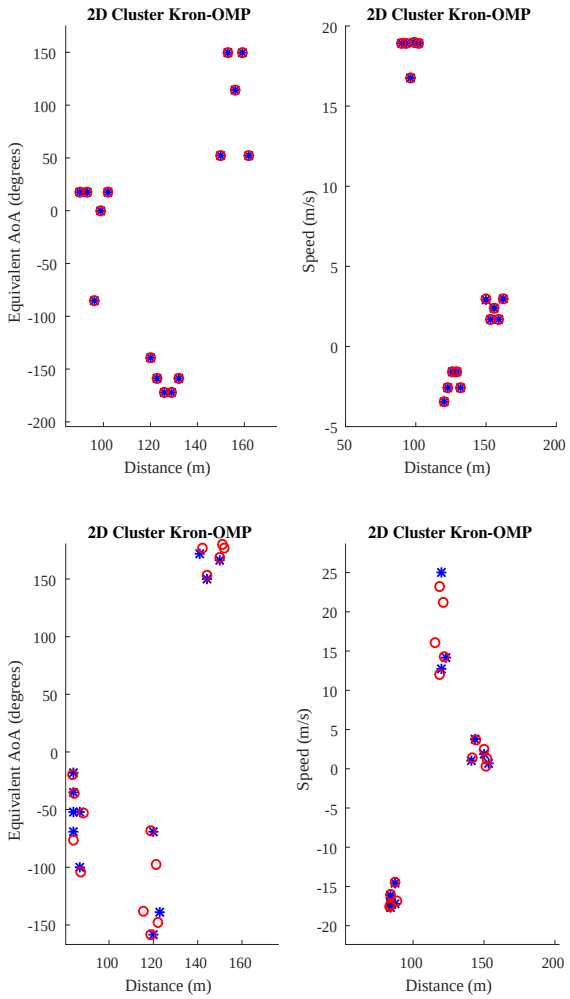

Fig. 8: Two random realizations of downlink sensing using the proposed 2D cluster kron-OMP algorithm for quantized (top sub-figures) and non-quantized (bottom sub-figures) channel parameters

Moreover, we do Monte-Carlo trials for both our proposed 2D cluster kron-OMP and conventional 2D kron-OMP for same non-quantized channel parameters with $N_s = 28$ DMRS subcarriers. Uplink sensing simulated for N_{iter} trails each time and we compute the Root-mean-square error (RMSE) for AoA estimates at each N_{iter} as,

$$RMSE_{AoA} = \sqrt{\frac{1}{(N_{iter}L)} \sum_{j=1}^{N_{iter}} \sum_{\ell=1}^{L} \left| \hat{\phi}_{\ell,j} - \phi_{\ell,j} \right|^2}. \quad (16)$$

AoA estimation performance is evaluated versus all N_{iter} iterations considered in the top figure and versus the number of clusters in channels with $N_{iter} = 100$ in the bottom figure of Fig. 11 respectively. The proposed 2D cluster kron-OMP algorithm achieves the best performance for all iterations in comparison with its cluster-less peer 2D kron-OMP. In addition, as we increase the number of clusters in Cluster-Chl, we can also observe relatively better estimation in the proposed algorithm.

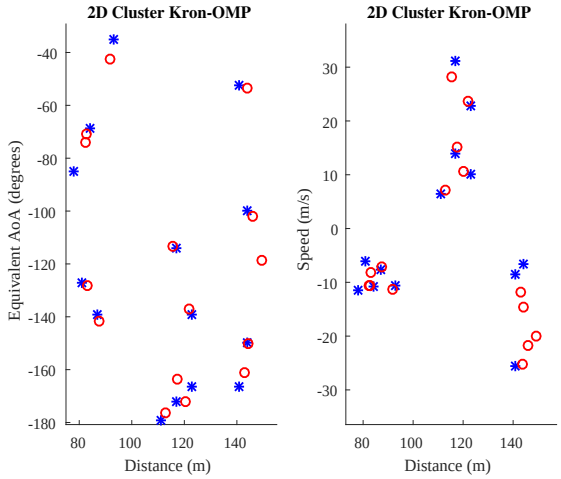

Fig. 9: A random realization of uplink sensing using the proposed 2D cluster kron-OMP algorithm for non-quantized channel parameters

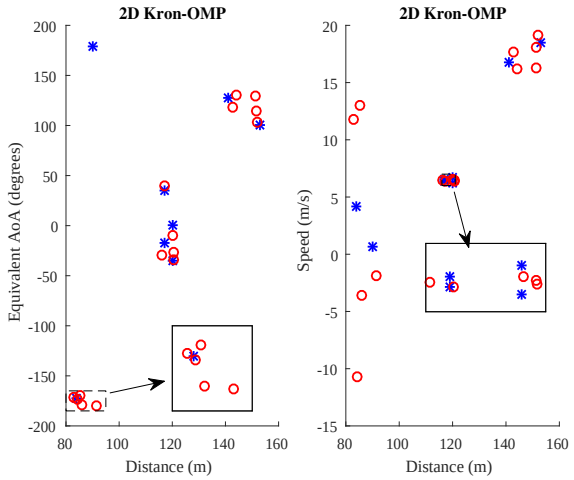

Fig. 10: Uplink sensing using conventional 2D kron-OMP for non-quantized channel parameters with $N_s = 28$ DMRS subcarriers. Black zoomed in boxes are for showing certain missed estimates incapability of preserving cluster pattern

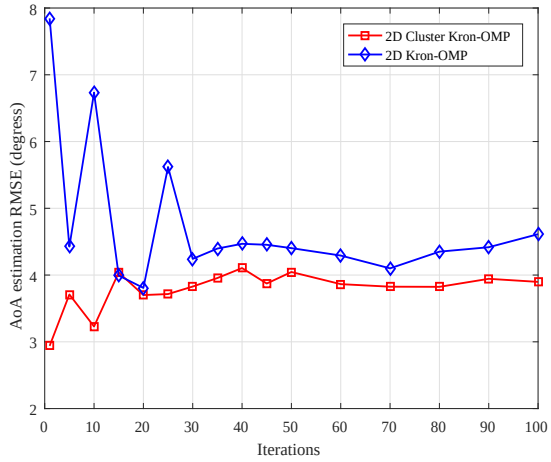

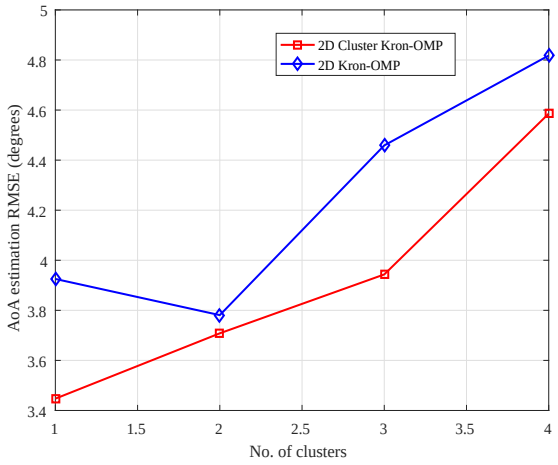

Fig. 11: RMSE of the AoA estimates obtained by both methods with $N_s = 28$ for non-quantized channel parameters

C. Comparative Study on Simulation Results

Existing algorithms have respective shortcomings for sensing parameter estimation in perceptive mobile networks, as compared with the proposed methods and the comparative study obtained from the simulation results is given in Table I. Generally, the classical 2D DFT method is simple and less complex but this provides low resolution and requires a full set of measurements in time or frequency domain. Again, in ESPRIT and MUSIC, the reasonable resolution requires at least a large segment of consecutive samples and this is not always available in uplink sensing. In contrast, off-grid type compressive methods do not require consecutive samples but implementation for real time operation imposes high complexity. Moreover, off-grid CS contain respective constraints on the parameter estimation range and the minimum separation of the parameter values [1]. We rather establish the received signals to an arrangement such that from it any of the methods in 1D-3D CS algorithms can be functional to acquire the estimates for the sensing parameters from the linked sparse reconstructed estimates corresponding to the utilized dictionaries.

Normally, higher-dimensional CS algorithms achieve better estimation performance with the price of much higher computational complexity. The sensing problem becomes more critical when the number of measurements is limited because of the short channel coherent time and a small number of antennas in the perceptive mobile network. In the case of using on-grid CS methods, the number of available observations in the selected dimension plays an important role in dominating the estimation accuracy and resolution. The lack of sufficient measurements in each dimension could likely create large quantization errors even using high-dimensional on-grid CS algorithms such as the Tensor tool and Kronecker CS in the domains of Doppler frequency, AoD and AoA. Fortunately, the cellular signals usually have hundreds to thousands of subcarriers, which provide numerous measurements for the delay. Therefore, quantizing the only delay can hypothetically lead to reduced errors. In particular in the 2D cluster kron-OMP, the cluster prior probability density function that introduced with the CS reconstruction algorithm, efficiently

detect the coarse locations of the clusters, leading to more accurate sparse reconstruction performance when 2D Kron CS algorithms are applied.

VI. Conclusion

In this paper, we focus on JCAS techniques that are related and tailored to cellular/mobile networks, which is also the main differentiator of this paper to other existing ones. We presented three preliminary sensing algorithms using 1D, 2D and 3D compressive sensing algorithms, and provided simulation results, using channels generated from both our cluster model and 5G QuaDRiGa channel model. These results indicate that reasonable sensing performance can be achieved, and demonstrate the respective advantages and disadvantages of these algorithms. We also compare our 1D to 3D results with the cases when the occupied subcarrier is less in uplink and with the results from 2D discrete Fourier transform. Our work also disclosed some interesting research problems to work on as future works, such as the ambiguity problem due to interleaved subcarriers and reduced resolution in 3D CS algorithms. We have proposed a 2D cluster Kronecker OMP algorithm for sensing parameter estimation in perceptive mobile networks, which can exploit the cluster structure in multipath channels. By introducing a cluster prior, our algorithm can efficiently detect the coarse locations of the clusters, leading to more accurate sparse reconstruction performance when block CS algorithms are applied. The estimation accuracy of the 2D cluster Kronecker OMP algorithm in terms of mean squared error is also shown in comparison with the one without cluster prior. We further explain the distinctions between the proposed algorithms to give a comparison between this work and other sensing schemes. Simulation results demonstrate that our proposed algorithm can achieve better parameter estimation accuracy, for both on-grid and off-grid channel models, compared to the scheme without using prior knowledge.

VII. Acknowledgments

This work is partially financially supported by China Academy of Telecommunications Technology (CATT), China.

References

[1] Rahman, M.L., Zhang, J.A., Huang, X., Guo, Y.J., Heath Jr, R.W.: 'Framework for a perceptive mobile network using joint communication and radar sensing', *IEEE Transactions on Aerospace and Electronic Systems*, 2019, pp. 1–1

[2] Rahman, M.L., Cui, P., Zhang, J.A., Huang, X., Guo, Y.J., Lu, Z. 'Joint communication and radar sensing in 5G mobile network by compressive sensing'. In: 2019 19th International Symposium on Communications and Information Technologies (ISCIT). (Vietnam, 2019). pp. 599–604

[3] Zhang, J.A., Cantoni, A., Huang, X., Guo, Y.J., Heath, R.W. 'Framework for an innovative perceptive mobile network using joint communication and sensing'. In: 2017 IEEE 85th Vehicular Technology Conference (VTC Spring). (Sydney, Australia, 2017). pp. 1–5

[4] Zhang, J.A., Huang, X., and, Y.J.G., Rahman, M.L. 'Signal Stripping Based Sensing Parameter Estimation in Perceptive Mobile Networks'. In: 2017 IEEE-APS Topical Conference on Antennas and Propagation in Wireless Communications (APWC). (Italy, 2017). pp. 67–70

[5] Martone, A.F., Gallagher, K.A., Sherbondy, K.D. 'Joint radar and communication system optimization for spectrum sharing'. In: 2019 IEEE Radar Conference (RadarConf). (Boston, 2019). pp. 1–6

[6] Liu, F., Masouros, C., Li, A., Sun, H., Hanzo, L.: 'MU-MIMO communications with MIMO Radar: From co-existence to joint transmission', *IEEE Transactions on Wireless Communications*, 2018, **17**, (4), pp. 2755–2770

[7] Saruthirathanaworakun, R., Peha, J.M., Correia, L.M.: 'Opportunistic sharing between rotating radar and cellular', *IEEE Journal on Selected Areas in Communications*, 2012, **30**, (10), pp. 1900–1910

[8] Chiriyath, A.R., Paul, B., Bliss, D.W.: 'Radar-Communications Convergence: Coexistence, Cooperation, and Co-Design', *IEEE Transactions on Cognitive Communications and Networking*, 2017, **3**, (1), pp. 1–12

[9] Zheng, L., Lops, M., Eldar, Y.C., Wang, X.: 'Radar and communication coexistence: An overview: A review of recent methods', *IEEE Signal Processing Magazine*, 2019, **36**, (5), pp. 85–99

[10] Rossler, C.W., Ertin, E., Moses, R.L. 'A software defined radar system for joint communication and sensing'. In: 2011 IEEE Radar Conference (RADAR). (IEEE, 2011. pp. 1050–1055

[11] Hassanien, A., Himed, B., Amin, M.G. 'Transmit/receive beamforming design for joint radar and communication systems'. In: 2018 IEEE Radar Conference (RadarConf18). (Oklahoma City, 2018). pp. 1481–1486

[12] Sturm, C., Wiesbeck, W.: 'Waveform Design and Signal Processing Aspects for Fusion of Wireless Communications and Radar Sensing', *Proceedings of the IEEE*, 2011, **99**, (7), pp. 1236–1259

[13] Kumari, P., Choi, J., Prelcic, N.G., Heath, R.W.: 'IEEE 802.11ad-based Radar: An Approach to Joint Vehicular Communication-Radar System', *IEEE Transactions on Vehicular Technology*, 2017, **PP**, (99), pp. 1–1

[14] Braun, M. 'OFDM Radar Algorithms in Mobile Communication Networks' [PhD Thesis]. Karlsruher Institut f˙ur Technologie (KIT), 2014

[15] Wang, X., Hassanien, A., Amin, M.G.: 'Dual-function MIMO radar communications system design via sparse array optimization', *IEEE Trans Aerospace and Electronic Systems*, 2019, **55**, (3), pp. 1213–1226

[16] Rong, Y., Chiriyath, A.R., Bliss, D.W. 'Multiple-antenna multiple-access joint radar and communications systems performance bounds'. In: 2017 51st Asilomar Conference on Signals, Systems, and Computers. (Pacific Grove, CA, USA, 2017). pp. 1296–1300

[17] Liu, Y., Liao, G., Xu, J., Yang, Z., Zhang, Y.: 'Adaptive OFDM integrated radar and communications waveform design based on information theory', *IEEE Communications Letters*, 2017, **21**, (10), pp. 2174–2177

[18] Friedlander, B.: 'Waveform design for MIMO radars', *IEEE Transactions on Aerospace and Electronic Systems*, 2007, **43**, (3), pp. 1227–1238

[19] Hack, D.E., Patton, L.K., Himed, B., Saville, M.A.: 'Detection in passive mimo radar networks', *IEEE Transactions on Signal Processing*, 2014, **62**, (11), pp. 2999–3012

[20] Zheng, L., Wang, X.: 'Super-resolution delay-doppler estimation for OFDM passive radar', *IEEE Transactions on Signal Processing*, 2017, **65**, (9), pp. 2197–2210

[21] 3GPP TR 38. 913: 'Study on scenarios and requirements for next generation access technologies', *V1500*, June 2018,

[22] Lim, C.W., Wakin, M.B. 'Recovery of periodic clustered sparse signals from compressive measurements'. In: 2014 IEEE Global Conference on Signal and Information Processing (GlobalSIP). (Atlanta, 2014). pp. 409–413

[23] Yu, L., Sun, H., Zheng, G., Pierre.Barbot, J.: 'Model based bayesian compressive sensing via local beta process', *Signal Process*, 2015, **108**, (C), pp. 259–271

[24] Yu, L., Wei, C., Jia, J., Sun, H.: 'Compressive sensing for cluster structured sparse signals: variational bayes approach', *IET Signal Processing*, 2016, **10**, (7), pp. 770–779

[25] Zhang, Z., Rao, B.D. 'Recovery of block sparse signals using the framework of block sparse bayesian learning'. In: 2012 IEEE International Conference on Acoustics, Speech and Signal Processing (ICASSP). (Kyoto, Japan, 2012. pp. 3345–3348

[26] Jiao, C., Zhang, Z., Zhong, C., Feng, Z. 'An indoor mmwave joint radar and communication system with active channel perception'. In: 2018 IEEE International Conference on Communications (ICC). (Kansas City, USA, 2018). pp. 1–6

[27] 3GPP TS 38. 211: 'Physical channels and modulation', *V1520*, July 2018,

[28] Shutin, D. 'Cluster analysis of wireless channel impulse responses'. In: International Zurich Seminar on Communications, 2004. (Zurich, Switzerland, 2004). pp. 124–127

[29] Ji, S., Xue, Y., Carin, L.: 'Bayesian compressive sensing', *IEEE Transactions on Signal Processing*, 2008, **56**, (6), pp. 2346–2356

[30] Duarte, M.F., Baraniuk, R.G.: 'Kronecker compressive sensing', *IEEE Transactions on Image Processing*, 2012, **21**, (2), pp. 494–504

TABLE I: Comparison of sensing results obtained from various sensing algorithms

Methods	Suitability	Main Limitation
1D CS	Estimated points are well matched with three clusters with few extra points due to residual in threshold	In case with limited DMRS, the shape still well maintained, however,resolution ambiguity problem in delay.
2D Kron CS	Estimated values are in closer vicinity with actual clustered multipath values (AoA) in comparison with 1D.	Interleaved subcarriers in this case actually cause ambiguity in estimation.
3D Tensor CS	Coarse estimation in both AoA and speed domains; estimation results is not as good as 1D and 2D algorithms.	It involves much higher computational complexity. Moreover, the interleaved subcarriers may cause near-singular matrix. Random subcarrier allocation is generally preferred in such case for improved estimation.
2D DFT	Provides reliable and simple coarse estimates, but the resolution is very low in comparison with all results of 1D-3D CS	Generally, requires a full set of measurements in time or frequency domain, which may not be satisfied in uplink sensing.
2D cluster kron-OMP	The estimates preserve the cluster structure and convey correct information for determining the location and moving speed of the scatters.	For continuous off-grid parameters, performance degradation can be observed with reduced accuracy and missed estimates.

[31] Caiafa, C.F., Cichocki, A.: 'Computing sparse representations of multidimensional signals using kronecker bases', *Neural Computation*, 2013, **25**, (1), pp. 186–220

[32] Grant, C.S., Moon, T.K., Gunther, J.H., Stites, M.R., Williams, G.P.: 'Detection of amorphously shaped objects using spatial information detection enhancement (SIDE)', *IEEE Journal of Selected Topics in Applied Earth Observations and Remote Sensing*, 2012, **5**, (2), pp. 478–487

[33] Yu, L., Sun, H., Barbot, J.P., Zheng, G.: 'Bayesian compressive sensing for cluster structured sparse signals', *Signal Processing*, 2012, **92**, (1), pp. 259 – 269

[34] Shekaramiz, M., Moon, T.K., Gunther, J.H.: 'Bayesian compressive sensing of sparse signals with unknown clustering patterns', *Entropy*, 2019, **21**, (3)

[35] Bader, B.W., Kolda, T.G.: 'Efficient MATLAB computations with sparse and factored tensors', *SIAM Journal on Scientific Computing*, 2007, **30**, (1), pp. 205–231

[36] Hakobyan, G., Yang, B. 'A novel OFDM-MIMO radar with non-equidistant subcarrier interleaving and compressed sensing'. In: 2016 17th International Radar Symposium (IRS). (Krakow, Poland, 2016). pp. 1–5